ELSEVIER

Chemical Engineering Journal 126 (2007) 23–33

Chemical Engineering Journal

www.elsevier.com/locate/cej

The effect of electrolytes on the critical velocity for bubble coalescence

Cláudio P. Ribeiro Jr. *, Dieter Mewes

Institute of Process Engineering, University of Hannover, Callinstrasse 36, 30167 Hannover, Germany

Received 1 March 2006; received in revised form 28 August 2006; accepted 29 August 2006

Abstract

An experimental study concerning the influence of electrolytes on the critical velocity for bubble coalescence is presented. Bubble collisions in water and two NaCl solutions (0.100 and 0.300 wt%) were recorded with a high-speed video camera at four different operating temperatures ($10 \leq T_L \leq 40\,^{\circ}C$), using air as the dispersed phase in all cases. For all operating conditions analysed, the critical velocity was observed to be initially a decreasing function of the equivalent diameter of the colliding bubbles up to a given value, at which it became constant. This behaviour was physically reasoned in terms of the importance of bubble deformation during the drainage of the liquid film between the bubbles. Regardless of the composition of the liquid phase, an increase in the liquid temperature enhanced bubble coalescence. An empirical equation including three parameters was proposed to describe the experimentally observed trends. Two parameters were only temperature-dependent and all electrolytes effects were hence lumped together in the third parameter.

Keywords: Bubbles; Coalescence; Bouncing; Electrolytes; Bubble columns; Direct-contact evaporators

1. Introduction

The dispersion of a gas into a liquid phase with or without suspend solids for promoting mass and/or heat transfer is a common step in both reactors and separation units from several industrial processes. Bubble columns, gas strippers, distillation towers, direct-contact evaporators, flotation columns and stirred aerated tanks are just some examples of important units which comprise the general class of gas–liquid contactors. In this kind of equipment, the transfer rates are closely related to and may even be controlled by the interfacial area, which therefore constitutes an important design parameter. The accurate determination of the interfacial area in gas–liquid systems is a challenging task, as this parameter depends on the frequency of break-up and coalescence of bubbles, complex phenomena whose mechanisms are still not fully understood [1,2]. Apart from its influence on the interfacial area, bubble coalescence, in particular, also plays an important role in the transition of flow regimes in bubble columns [3], as well as in the transient evolution of the overall gas hold-up in direct contact-evaporators [4].

Due to its importance for the performance of gas-liquid contactors, bubble coalescence has been the subject of intense research. Most of the past work can be divided into three subjects, namely, the development of film-drainage models [5–8], the physical understanding of the effects of surface active solutes [9–13] and the establishment of new experimental strategies for determining coalescence times or film thickness [14–17]. The number of available reports is drastically reduced when it comes to the role of the relative velocity of the approaching bubbles in the process.

The importance of the approach velocity for bubble coalescence was first pointed out by Kirkpatrick and Lockett [18]. Working with the air–water system and measuring the coalescence time between a bubble and a free interface, these authors demonstrated that the coalescence time was very small at a low approach velocity but increased significantly for large approach velocities. In agreement with these observations, Chesters and Hofman [19] stated that, due to the competition between the thinning of the liquid layer between two approaching bubbles and the increase in the free energy of the system on account of the increase in the surface area of the bubbles, there should be a critical Weber number for bubble coalescence defined in terms of the maximum relative velocity of the bubbles at which coalescence took place, the so-called critical velocity, u_c. These authors carried out a theoretical analysis of the flow and deformation of the liquid film between two bubbles in an inviscid liquid and proposed an equation for this critical Weber number, which was regarded as only qualitatively reliable due to many simplifica-

* Corresponding author. Tel.: +49 511 762 3860; fax: +49 511 762 3031.
E-mail address: cprj@peq.coppe.ufrj.br (C.P. Ribeiro Jr.).

1385-8947/$ – see front matter © 2006 Elsevier B.V. All rights reserved.
doi:10.1016/j.cej.2006.08.029

Nomenclature

d	bubble or drop diameter (m)
d_e	equivalent bubble diameter defined by Eq. (1) (m)
Eo	Eötvös number ($g(\rho_L - \rho_G)d^2\sigma^{-1}$)
F_{ol}	overlapping function defined by Eq. (2)
g	gravitational acceleration (m s^{-2})
n	number of collisions
Re	Reynolds number ($\rho_L U d\eta^{-1}$)
T	temperature (K)
u_c	critical velocity for coalescence (m s^{-1})
u_{rel}	relative velocity between bubbles (m s^{-1})
U	particle velocity (m s^{-1})
V	vector of experimental relative velocities of the bubble collisions (m s^{-1})

Greek symbols

α	empirical parameter in Eq. (6) related to the effect of d_e on u_c (s^{-1})
β	empirical parameter in Eq. (6) related to the effect of electrolytes on u_c (m s^{-1})
δ	empirical parameter in Eq. (6) associated with the minimum diameter for dimple formation (m)
η	viscosity (Pa s)
Λ	dimensionless extent of overlapping in the data set
μ	unit step function
$\mu^\bullet$	modified unit step function defined by Eq. (5)
ρ	density (kg m^{-3})
σ	surface tension (N m^{-1})

Subscripts

00	water
01	aqueous solution of NaCl 0.100 wt%
03	aqueous solution of NaCl 0.300 wt%
bou	bouncing
coal	coalescence
i	collision i
L	liquid
G	gas

Superscripts

exp	experimental
pred	predicted with Eq. (6)

tions involved in its deduction. Upon analysing the collision of equally sized pairs of bubbles in water, Duineveld [20] observed coalescence to take place whenever the Weber number based on the relative velocity of the bubbles, u_{rel}, was smaller than 0.18. However, Sanada et al. [21] have shown with their data for bubble coalescence in different silicone oils that the liquid kinematic viscosity is also important in the process, so that it would be more appropriate to speak of a critical Reynolds number. In a recent contribution, Ribeiro and Mewes [22] observed the critical velocity to grow linearly with the operating temperature, an effect whose intensity depended on the physical properties of the liquid phase. The data of Duineveld [20] and Sanada et al. [21], as well as those obtained by Wiemann [23] for suspensions of glass particles in water, were correlated by Ribeiro and Mewes [22] together with their own data for water and ethanol with a dimensionless equation in terms of a critical Reynolds number and a modified Morton number, whose mean deviation was equal to 10%.

Lehr et al. [24] recognised the modelling potential behind the concept of critical velocity and adopted it in the development of a coalescence kernel function. The basic idea was to use the values of u_c and u_{rel} to assess the coalescence efficiency, instead of the traditional option of film-drainage models and empirical parameters adopted in other kernel functions [25–28]. Utilising their u_c value determined for the air-water system, Lehr et al. [24] successfully adopted their kernel function in the numerical calculation of bubble-size distributions and flow fields in bubble columns. The flexibility of this kernel function was later on demonstrated by Wiemann [23], who studied the effect of suspended solids on the critical velocity and subsequently used his experimental u_c values in the kernel function of Lehr et al. [24] for simulating the dynamic operation of slurry bubble columns with and without mass transfer.

It is well known in the literature that the addition of most inorganic electrolytes into water brings about a significant reduction in bubble coalescence [4,9,10,29–32], which is usually indicated by the reduction in a previously defined coalescence frequency or by a reduction in the mean bubble diameter. Nonetheless, the important issue of how this coalescence hindrance is reflected in terms of the critical velocity has not been experimentally addressed so far. This would provide not only useful information to the establishment of a mechanism for the effect of electrolytes on bubble coalescence, but also the necessary data to enable the application of the kernel function of Lehr et al. [24], which, in turn, would provide the means for simulating, for instance, the dynamic operation of bubble columns fed with electrolyte solutions, a rather relevant issue in the case of bioreactors. Although true that an equation was proposed by Lehr et al. [24] to estimate u_c for aqueous electrolyte solutions involving the gas hold-up of small bubbles for developed flow in bubble columns operating with high gas superficial velocities, its predictions were not compared with experimental u_c values.

In view of the aforementioned considerations, we present here an experimental study on the influence of inorganic electrolytes on the critical velocity for bubble coalescence. Bubble collisions were recorded with the aid of a high-speed video camera in order to determine u_c values in aqueous NaCl solutions for two different salt concentrations (0.100 and 0.300 wt%) and four distinct operating temperatures ($10 \leq T_L \leq 40\,^\circ$C). In addition, experiments with distilled water at the same range of liquid temperature were carried out for comparison.

2. Experimental

All runs were carried out with the aid of the experimental set-up shown in Fig. 1. It basically consisted of the coalescence cell and a storage tank, 5.0 dm^3 in volume, provided with a

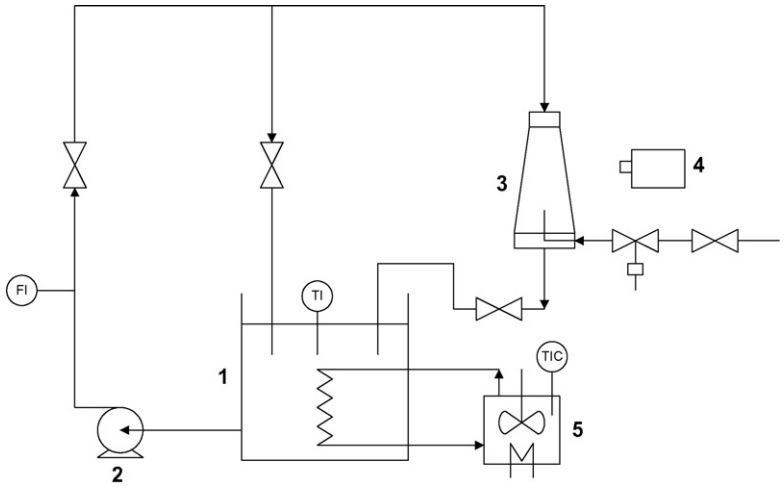

Fig. 1. Experimental set-up—(1) feed tank; (2) circulation pump; (3) coalescence cell; (4) high-speed camera; (5) temperature-controlled circulation bath.

heating/cooling element connected to a temperature-controlled circulation bath (Julabo® F10).

The coalescence cell was made of Plexiglas® and had a channel with rectangular cross section available for liquid flow. The liquid was fed at the top of the cell and flowed vertically downwards. In order to equalise the velocity profile throughout the cross section, an internal element with small hexagonal channels was placed at the entrance of the cell. The cross-section area for fluid flow widened from 24 mm × 5 mm at the entrance to 60 mm × 5 mm at the bottom, which brought about a reduction in the average liquid velocity along the direction of flow. The bubbles were injected by a capillary located at the bottom of the cell and their sizes could be varied according to the injected gas volume. During operation, the bubbles ascended through the countercurrently flowing liquid up to the point where an equilibrium between the interacting forces was achieved. On account of the reduced dimension of the cell's depth, bubble movements were basically restricted to two dimensions.

Compressed air was used as the dispersed phase in all runs. Double-distilled water (with an electrical conductivity equal to $2 \pm 1\ \mu S\ cm^{-1}$) and NaCl (99.8%, Carl Roth®) were utilised to prepare the solutions used as the continuous phase. Two different NaCl concentrations were considered, namely 0.100 and 0.300 wt%. In order to guarantee measurable coalescence during the experiments, the chosen NaCl concentrations were lower than the transition concentration of 0.145–0.175 mol dm^{-3} (0.85–1.02 wt%) reported for this electrolyte [9,33], at which the coalescence frequency is reduced to 50% of the value related to distilled water. The operating temperature, measured with the aid of a pre-calibrated platinum resistance thermometer (PT-100) located in the feed tank, was varied from 10 to 40 °C.

A high-speed video camera (Speedcam + 500, Weinberger®) provided with zoom lenses was employed to observe the motion of the bubbles, using a frame rate of 529 fps and a spatial resolution of 256 × 256 pixels. The pictures were analysed automatically with the aid of the software Image J [34], version 1.33h, according to the procedure detailed by Ribeiro and Mewes [22]. For each collision, the relative velocity of the bubbles perpendicular to the surface of contact and the size of the colliding bubbles were determined, the latter estimated as the diameter of the corresponding circle with the same area. In addition, it was visually detected whether the collision led to coalescence or bouncing. Bubble contours were automatically identified by the software and the estimated error for bubble sizes, based on measurements for different regions with the same area selected in the graduated scale of the pictures, is equal to about 1%. With regard to relative velocities, a somewhat higher error, equal to about 3%, is estimated, considering that data fitting was involved.

At the beginning of each run, the whole experimental apparatus was thoroughly cleaned by batch circulation of double-distilled water in closed circuit until the difference in the electrical conductivity between the inlet and outlet streams became lower than $1\ \mu S\ cm^{-1}$. In a last cleaning stage, the solution to be tested was circulated for 5 min in the whole experimental apparatus. This cleaning solution was then discharged and the storage tank was re-filled with fresh solution. The temperature in the heating/cooling bath was set to the required value and the liquid circulation pump was turned on. Time was allowed for the whole system to achieve thermal equilibrium before bubble collisions started to be recorded. Liquid temperature in the storage tank was monitored throughout the recording period and it was observed not to deviate more than 0.5 °C from its nominal value.

Taking into account the experimental results of Drogaris and Weiland [35], who demonstrated that, for bubbles with unequal sizes, the coalescence time lay closer to the value associated with the smaller bubble, the following equivalent diameter was adopted as the characteristic length scale for bubble coalescence:

$$d_e = 2\left(\frac{1}{d_1} + \frac{1}{d_2}\right)^{-1} \quad (1)$$

With regard to the critical velocity, its value has been often estimated [20,21,23,24] based on a visual inspection of the collisions data to evaluate the maximum relative velocity at which bubble coalescence took place. In this work, however, we shall apply the quantitative criterion for determining u_c proposed by Ribeiro and Mewes [22]. According to this criterion, for

each data set comprising n_{coal} coalescence collisions and n_{bou} bouncing collisions, whose corresponding relative velocities are respectively stored in the vectors V_{coal} and V_{bou}, the critical velocity is estimated as the value that minimises the so-called overlapping function, F_{ol}, defined as follows:

$$F_{ol}(u_c) = \Lambda_{coal}(u_c) + \Lambda_{bou}(u_c) \tag{2}$$

$$\Lambda_{coal}(u_c) = \sum_{j=1}^{n_{coal}} \frac{V_{coal,j} - u_c}{V_{coal,j}} \mu^{\bullet}(V_{coal,j} - u_c) \times \frac{\sum_{j=1}^{n_{coal}} \mu^{\bullet}(V_{coal,j} - u_c)}{n_{coal} - \sum_{j=1}^{n_{coal}} \mu^{\bullet}(V_{coal,j} - u_c)} \tag{3}$$

$$\Lambda_{bou}(u_c) = \sum_{i=1}^{n_{bou}} \frac{u_c - V_{bou,i}}{V_{bou,i}} \mu(u_c - V_{bou,i}) \times \frac{\sum_{i=1}^{n_{bou}} \mu(u_c - V_{bou,i})}{n_{bou} - \sum_{i=1}^{n_{bou}} \mu(u_c - V_{bou,i})} \tag{4}$$

where $\mu^{\bullet}(x)$ is the traditional unit step function and $\mu^{\bullet}(x)$ is a modified unit step function given by

$$\mu^{\bullet}(x) = \begin{cases} 0, & \text{if } x \le 0 \\ 1, & \text{if } x > 0 \end{cases} \tag{5}$$

For a given data set, the value of u_c which minimises Eq. (2) was computed with the aid of a self-developed FORTRAN® code that applies the direct search polytope algorithm implemented in the subroutine DUMPOL from the ISML library, whose tolerance was set to 10^{-10}.

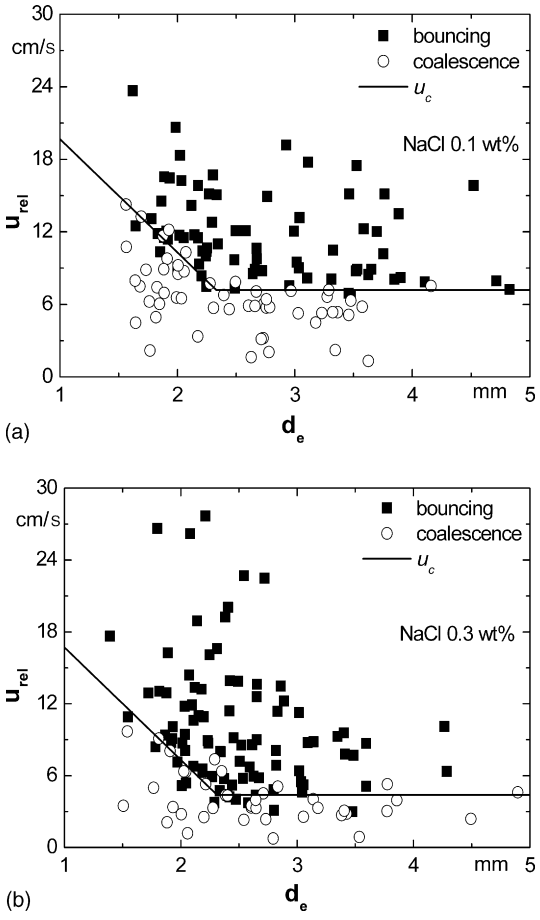

Fig. 2. Relatives velocities and outcomes of bubble collisions as a function of the equivalent diameter of the bubbles for 0.100 wt% (a) and 0.300 wt% (b) NaCl solutions at 21.0 °C.

3. Results and discussion

We shall start with an analysis of the results for the bubble collisions in the NaCl solutions at 21.0 °C. The bubble relative velocities for both coalescence and bouncing collisions at these operating conditions are plotted in Fig. 2 as a function of the equivalent diameter of the bubbles. Regardless of the electrolyte concentration, two distinct regions are identified in the data sets. In the first one, the boundary between bouncing and coalescence collisions does not seem to depend on d_e, which is in agreement with previous literature results for both water [22–24] and suspensions of glass particles in water [23]. The relative velocity associated with this boundary is clearly smaller than the critical velocity of 9.57 cm s^{-1} reported by Ribeiro and Mewes [22] for water. Moreover, it decreased as the NaCl concentration was raised. Both observations are consonant with the coalescence hindrance brought about by electrolytes in water. Nevertheless, in the second region of the data sets, which approximately corresponds to $d_e < 2.3$ mm, the boundary between coalescence and bouncing starts to depend on the equivalent diameter of the colliding bubbles, and the smaller the bubbles, the higher the minimum values of relative velocities required for bouncing to occur. Such a behaviour was not reported in the previous works of Lehr et al. [24], Wiemann [23] and Ribeiro and Mewes [22], as all these authors restricted themselves to collisions with $d_e \ge 2.8$ mm. It is interesting to observe, in particular, that, in this second region, for both NaCl concentrations, coalescence was observed even when u_{rel} was greater than any u_c value previously reported in the literature [20,22–24] for water, which is certainly not in agreement with the expected coalescence hindrance effect of electrolytes.

Taking into account this apparent contradiction in the data obtained for the region of small bubbles, it was decided to perform experiments with pure distilled water, focusing now on collisions with $d_e \le 2.8$ mm. The results of our runs, together with those presented by Ribeiro and Mewes [22] for $d_e \ge 2.8$ mm, are shown in Fig. 3. Even though new data for collisions with $d_e \ge 2.8$ mm were also obtained in our tests, no distinction between the data sources was made in Fig. 3 for the sake of clearness. It can now be seen that the region in which the boundary between coalescence and bouncing actually depends on d_e does also exist for water and, therefore, it is not related to the presence of electrolytes whatsoever.

The data in Figs. 2 and 3 evidence that previous authors' conclusion of a critical velocity for bubble coalescence that is independent of the equivalent diameter of the bubbles is only partially valid. In order to account for the existence of the second region in Figs. 2 and 3, we propose a new relationship for the

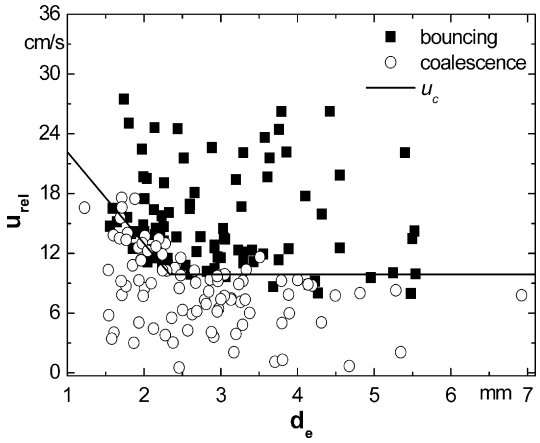

Fig. 3. Experimental results of this work and of Ribeiro and Mewes [22] for the outcome of bubble collisions in water at 21.0 °C.

critical velocity:

$$u_c(d_e) = \begin{cases} \alpha d_e + \beta & d_e \leq \delta \\ \alpha\delta + \beta & d_e > \delta \end{cases} \quad (6)$$

where α, β and δ are empirical parameters whose values have to be estimated based on experimental data. These parameters can be estimated by substituting Eq. (6) into Eq. (2) and calculating the corresponding minimum for the overlapping function. This procedure was adopted for each of the previous data sets and the obtained parameters were used to compute the continuous lines presented in Figs. 2 and 3. In each case, at least 20 different initial estimates of the parameters set were tested to avoid the computation of a local minimum. It can be seen that the proposed equation provides an appropriate description of the experimentally observed behaviour in these systems. For instance, using Eq. (6) and the whole data set in Fig. 3, the critical velocity predicted for $d_e > \delta$ is equal to 9.91 cm s^{-1}, a value which is less than 4% greater than the one reported by Ribeiro and Mewes [22].

The data related to the other operating temperatures considered in this work are plotted in Figs. 4–6 for water and the NaCl solutions. In the case of water, apart from our own results, the data of Ribeiro and Mewes [22] for $d_e \geq 2.8$ mm were also included in the graphs, even though, once again, a distinction of data sources was omitted for the sake of clearness. In all cases, the boundary between coalescence and bouncing collisions, that is, the critical velocity, is initially a decreasing function of the equivalent diameter, up to a specific point at which u_c becomes constant. Furthermore, for each liquid phase, a comparison of the data obtained for different temperatures indicates that the influence of the bubble diameter on the critical velocity decreases as the operating temperature is raised. All these trends are well represented by Eq. (6), whose parameters were estimated for each data set and the corresponding calculated values of u_c are shown as continuous lines in Figs. 4–6.

There are some experimental results in the literature that are consonant with this tendency verified in Figs. 2–6 of an increase in the coalescence probability as the bubbles become smaller for

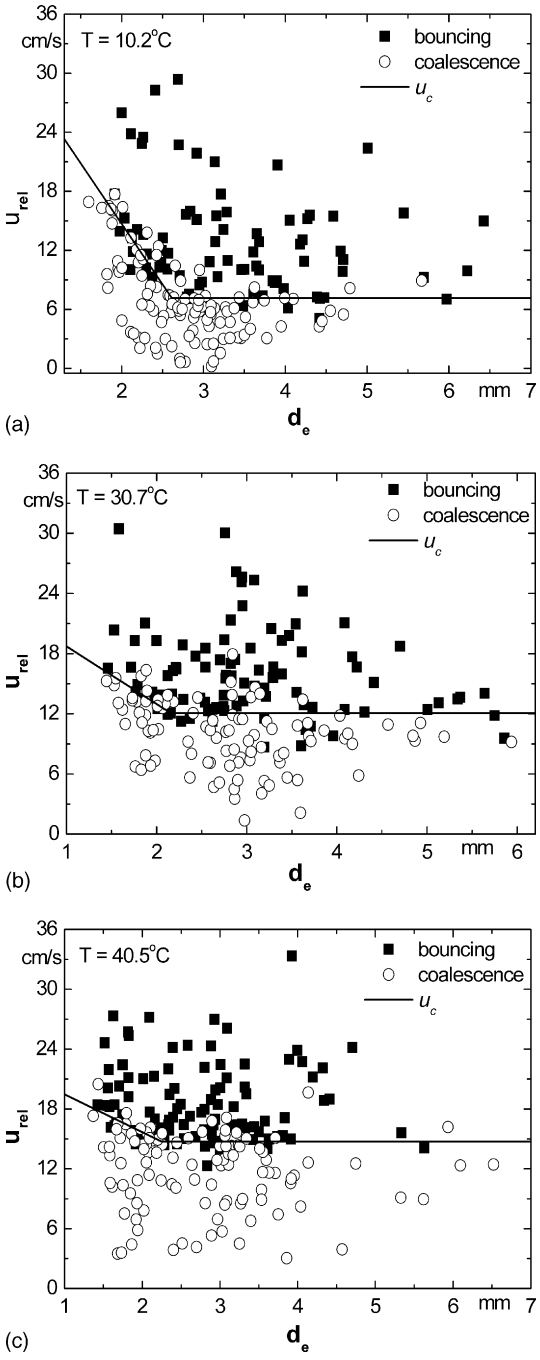

Fig. 4. Outcome of bubble collisions with different relative velocities as a function of the equivalent diameter of the bubbles in water at different temperatures: (a) 10.2 °C; (b) 30.7 °C; (c) 40.5 °C.

a certain range of bubble sizes. A significant increase in the coalescence time with the drop diameter was reported by Hodgson and Lee [36] for the water-toluene system ($d \leq 2.6$ mm), a trend that was also verified by Drogaris and Weiland [37] for air bubbles ($d \leq 3.9$ mm) in aqueous solutions of *n*-alcohols and fatty acids. Similarly, Doubliez [16] observed the thinning rate of the liquid film between a bubble ($d < 1.0$ mm) and a free surface to decrease with increasing bubble diameter in both water and aqueous solutions of alcohols (ethanol and methanol). In addition, Kok [38] and Duineveld [20] analysed buoyancy-driven

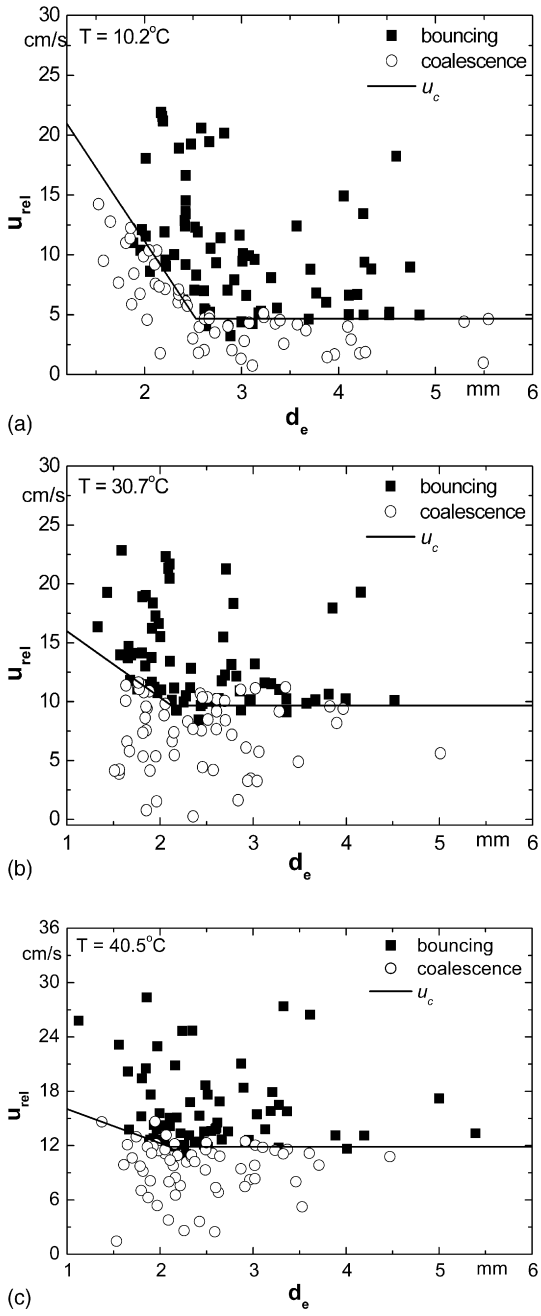

Fig. 5. Outcome of bubble collisions with different relative velocities as a function of the equivalent diameter of the bubbles in an aqueous NaCl solution 0.100 wt% for different temperatures: (a) 10.2 °C; (b) 30.7 °C; (c) 40.5 °C.

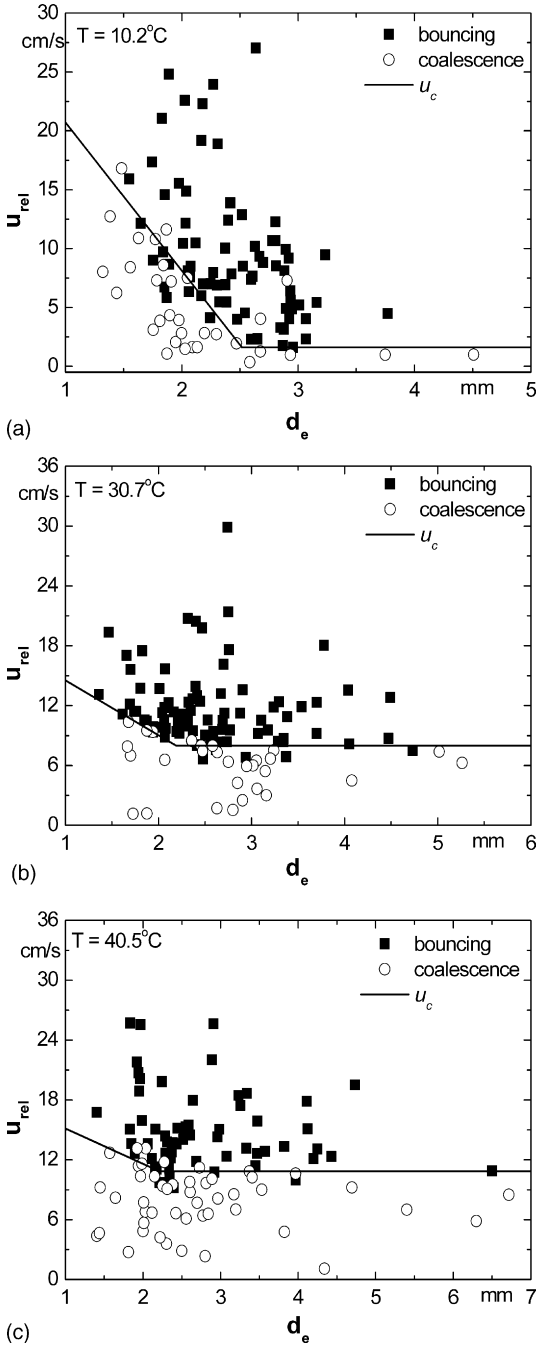

Fig. 6. Outcome of bubble collisions with different relative velocities as a function of the equivalent diameter of the bubbles in an aqueous NaCl solution 0.300 wt% for different temperatures: (a) 10.2 °C; (b) 30.7 °C; (c) 40.5 °C.

collisions of pair of gas bubbles and found coalescence in pure water to occur for all relative velocities tested when $d = 1.00$ mm and $d < 1.42$ mm, respectively. It should be noted that, according to the data presented by Clift et al. [39], for $1.00 \leq d \leq 1.42$ mm, the terminal velocity of air bubbles in water at 20 °C may vary from 9 to about 30 cm s^{-1}. Furthermore, for both electrolyte [40] and organic solutes [35], the concentration of solute required to produce a 50% reduction in the coalescence frequency in relation to water was observed to increase upon a decrease in the bubble diameter.

Even though Eq. (6) is empirical, the existence of two different regions in Figs. 2–6 can be physically reasoned. Bubble coalescence occurs when the interaction time between two approaching bubbles, which is a function of their relative velocity, is greater than the time required to drain the thin liquid film between them. Experimental evidence [16,36,37,41] and theoretical results from film-drainage models [5–8] indicate that the rate of drainage of the liquid film between two approaching bubbles or drops decreases as their size grows due to an increase in the area of drainage of the film.

The numerical study of the bubble bouncing with a free surface performed by Sanada et al. [21] demonstrates that for low relative velocities, the thickness of the liquid film is minimum at the bubble top and gradually increases towards the peripherals, with a corresponding pressure decrease in the same direction, whereas, as the bubble velocity increases, the liquid film becomes thicker at the bubble top than in the peripherals, with the formation of the characteristic liquid film shape known as dimple. In this case, a comparatively constant pressure distribution in the liquid film is obtained and the shape of the dimple actually prevents the bulk of the liquid from flowing out of the liquid film. Consequently, the dimple formation seems to be the main responsible for the existence of a critical velocity for bubble coalescence.

The formation of the dimple requires bubble deformation, which becomes more difficult as the bubbles get smaller, since the force required to produce a given distortion in a fluid particle increases with its curvature [41]. This fact is clearly illustrated in the work of Smolianski et al. [42], who simulated the coalescence of two bubbles in different shape regimes. For the coalescence of two spherical bubbles ($Re = 2$, Eo = 1.2), the liquid was quickly squeezed out of the space between the bubbles due to the considerable rigidity of the bottom of the upper bubble. However, in the case of ellipsoidal bubbles ($Re = 20$, Eo = 1.2), the bottom of the upper bubble deformed and a thin liquid film between the bubbles was formed. The upper bubble developed a dimpled-ellipsoidal shape and it was only when the bottom of the upper bubble could not deform any more that the liquid film between the bubbles started to get thinner.

Taking the previous aspects into account, the two regions in Figs. 2–6 may be related to two different film-drainage processes. In the first region, due to the small size of the bubbles, their curvature is too large for bubble deformation to be important. As a result, film drainage takes place without the formation of the dimple. Since the film-drainage time increases with the bubble diameter, the larger the equivalent diameter of the colliding bubbles, the longer the minimum interaction time for coalescence to take place, or, in other words, the lower the critical velocity for bubble coalescence. As the bubbles become larger, their curvature, equal to $1/d$ for spherical particles, falls rapidly, so that deformation is favoured, and there comes a point when the dimple is formed for the first time. From this point on, the changes in the curvature of the bubbles produced by further increases in their diameter become progressively less pronounced, and, accordingly, the minimum relative velocity required for the dimple formation tends to stabilise. The coalescence time stills increases with the bubble diameter, but now, on account of the possibility of deformation, the interaction time should also increase with the bubble size for a given relative velocity, so that a constant critical velocity for bubble coalescence is observed.

According to this reasoning, the point at which u_c starts to depend on the equivalent diameter would vary for each liquid, inasmuch as the bubble rigidity is related to the surface tension. The lower the surface tension, the smaller the bubble size required to obtain a curvature large enough for subsiding the importance of bubble deformation. In perfect agreement with this prediction, when working with ethanol as the continuous phase, whose surface tension is much smaller than the one associated with water, Ribeiro and Mewes [22] found no evidence of an equivalent-diameter-dependent critical velocity in the range $1.8 \leq d_e\ (\text{mm}) \leq 5.0$.

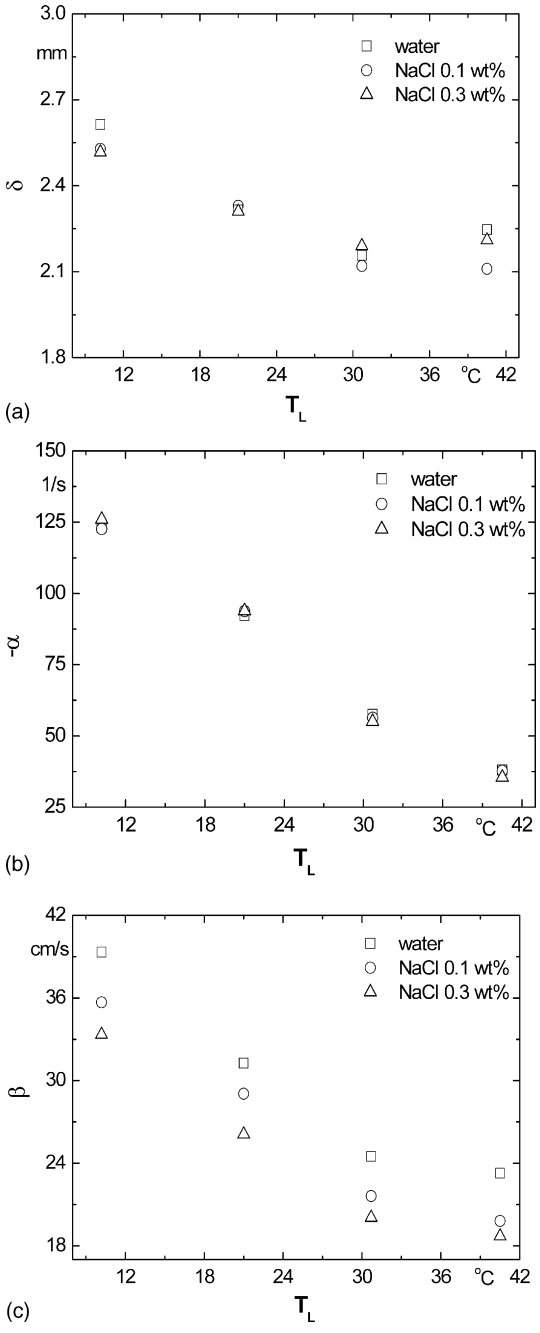

Fig. 7. Comparison of the parameters of Eq. (6) obtained in the individual fittings for each data set.

In order to get more insight into the behaviour of the parameters of Eq. (6) and their physical meaning, a comparison is drawn in Fig. 7 between the values obtained from the individual fittings for each operating condition considered. Starting with the parameter δ, the data in Fig. 7a demonstrate that the values obtained for the three different liquids at a given temperature are similar. Moreover, no straight correlation between the elec-

trolyte concentration and the value of δ was verified, that is, maximum and minimum values for each temperature were associated with different liquids. Therefore, within the adopted range of electrolyte concentrations, it seems that δ is not affected by the presence of electrolytes. Based on this conclusion, the different values for the three liquids tested can be now viewed as different estimates of a single parameter. Consequently, a clear drop is noticed in the value of δ as the temperature is raised from 10.2 to 30.7 °C, but a further increase in temperature does not cause changes in δ.

According to the physical reasoning used to understand the two regions in Figs. 2–6, the parameter δ would represent the minimum diameter for bubble deformation to play an important role in the film thinning process. Hence, its value would be sensitive to changes in the rigidity of the bubbles, and, more precisely, in the surface tension. According to the experimental data of Weissenborn and Pugh [43], at 21 °C, a maximum increase of about 0.11 mN m^{-1} in the surface tension of water is to be expected for the higher NaCl concentration adopted in this work, which is consonant with the fact that δ was independent of the composition of the liquid phase. The drop in surface tension with increasing temperature lessens the rigidity of the bubble for a given diameter, favouring bubble deformation and thereby reducing the value of δ. Considering that liquid viscosity considerably decreases as the temperature grows, the degree of deformation in the dimple required to suppress bubble coalescence is expected to increase with the operating temperature. The competition between these two opposite effects may be the reason for the stabilisation of δ after $T_L = 30.7$ °C.

Focusing now on α, as shown in Fig. 7b, the individual values for water and the two NaCl solutions at a given temperature are almost identical, which plainly suggests this parameter be independent of the electrolyte concentration within the investigated range. In addition, a significant drop in α upon an increase in the liquid temperature is noticed. In Eq. (6), α is the derivative of u_c with respect to d_e. It represents a lumped parameter to account for all processes which lead to the influence of the equivalent diameter on the critical velocity. As a result, a physical interpretation of the effect of T_L on α is by no means straightforward. We shall limit ourselves to the observation that, since the existence of the dependence of u_c upon d_e was reasoned in terms of a film-thinning process in which the curvature of the bubbles was too large for deformation to be important, one should expect this dependence to become less significant, and hence the value of α to fall, as the bubbles rigidity decreases, which is precisely what occurs with an increasing temperature due to the reduction in the surface tension.

As far as the third and last parameter of Eq. (6) is concerned, the data in Fig. 7c reveal that, similarly to what occurred to α, β is a decreasing function of the liquid temperature. The new and interesting aspect in this case is the fact that, contrary to the other two parameters in Eq. (6), β is a function of the electrolyte concentration. Thus, β constitutes a lumped parameter that describes the effect of electrolytes on the critical velocity in the proposed model.

Although true that the significant reduction in bubble coalescence promoted by the addition of most electrolytes into water constitutes a well-known fact in the literature, the actual mechanism responsible for such effect is not completely understood and, consequently, it seems difficult to develop a physical reasoning for the trends verified in Fig. 7c. Different theories have already been proposed to explain the effect of electrolytes on bubble coalescence, including the increase in the viscosity of the solution combined with changes in the water molecular structure caused by the presence of the solute [9], the increase in the elasticity of the liquid film [5,44], a reduction of the so-called hydrophobic force of attraction responsible for bubble coalescence [10], the decrease in the amount of dissolved gas in the solution [11] and electrostatic effects [12]. All theories, however, have their limitations and fail to explain some experimentally observed trend, as discussed by Deschenes et al. [13].

In view of the fact that the results of the individual fittings indicated the parameters δ and α to be independent of the electrolytes concentration, it was decided to conduct a new estimation of the parameters from Eq. (6). This time, for each of the two smallest operating temperatures, the data related to the three different liquids were used simultaneously in a single fitting for the estimation of five parameters, namely α, δ and one different β value for each liquid. Since there was no evidence in the individual fittings that the parameter δ should have different values at 30.7 and 40.5 °C, the data related to these two temperatures were considered simultaneously in a single fitting for the estimation of nine parameters: δ, one distinct α for each temperature and one different β for each pair temperature-electrolyte concentration. In each case, several initial estimates of the parameters set, including the values obtained in the individual fittings, were tested to avoid the computation of a local minimum. Such estimation procedures might not result in many an improvement in the case of the values of β, but are certainly useful to reduce the uncertain for both δ and α on account of the substantial increase in the number of data used in their estimation. The final values of the parameters estimated according to these procedures are listed in Table 1.

With the aim of assessing the quality of these new fittings, for a given experimental bubble collision, the equivalent diameter was used in Eq. (6) to compute the corresponding critical velocity with the proper set of parameters from Table 1 depending on the operating temperature and the electrolyte concentration, so that the ratio between the experimental u_{rel} and the predicted u_c could be calculated. The natural logarithm of the obtained ratios is plotted in Fig. 8 as a function of the equivalent diameter

Table 1
Empirical parameters for computing the critical velocity with Eq. (6) estimated considering simultaneously, for each temperature, the data for water and the NaCl solutions

Parameters	Liquid temperature (°C)			
	10.2	21.0	30.7	40.5
δ (mm)	2.710	2.447	2.182	2.182
α (s^{-1})	−92.59	−64.30	−50.54	−30.80
β_{00} (cm s^{-1})	32.31	25.64	23.13	21.65
β_{01} (cm s^{-1})	29.64	22.96	20.67	18.45
β_{03} (cm s^{-1})	26.09	19.78	19.02	17.74

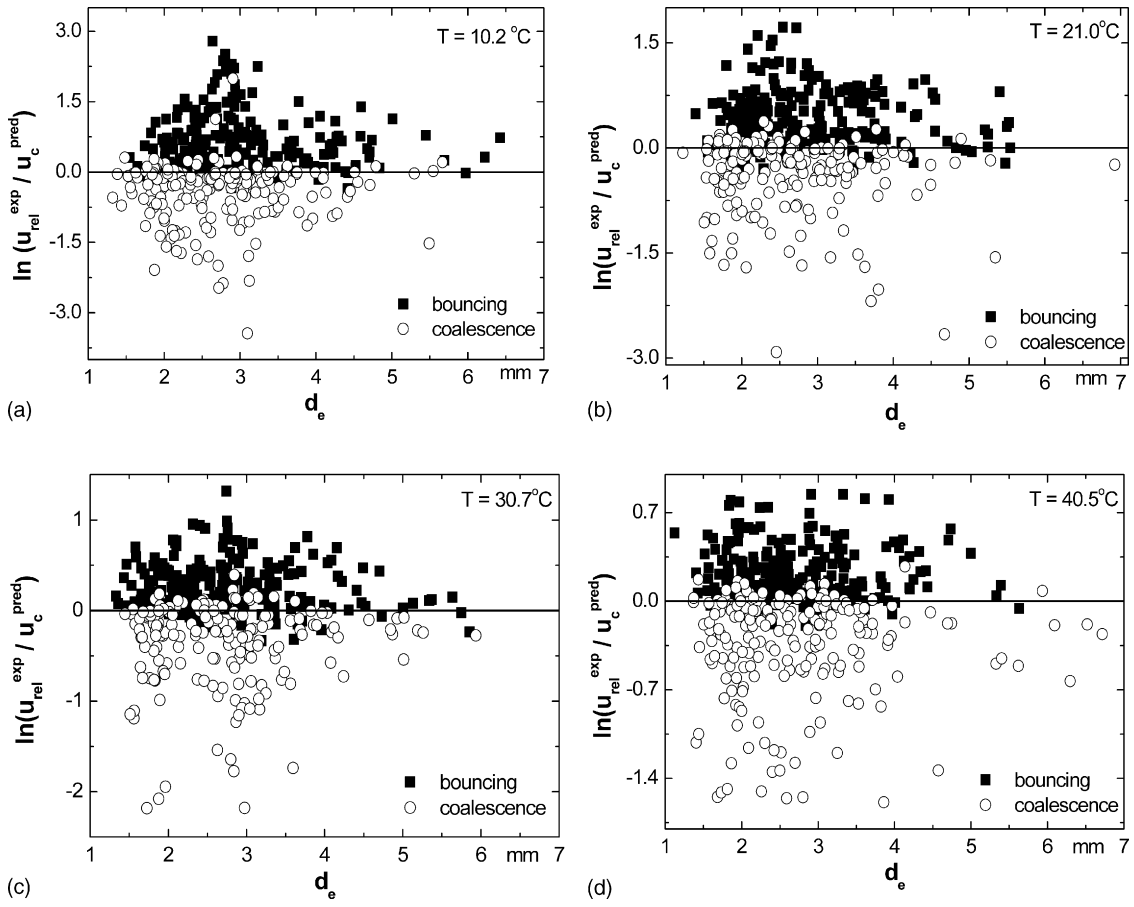

Fig. 8. Ratio of the experimental relative velocity to the critical velocity calculated with Eq. (6) and the parameters from Table 1 as a function of the equivalent diameter of the bubbles for the different liquid temperatures tested.

for the four operating temperatures analysed. Regardless of the liquid temperature, the data in Fig. 8 demonstrate that the fitted model provides a good description of the experimental data, since $u_{rel}^{exp}/u_c^{pred} \leq 1$ for the vast majority of the coalescence collisions and $u_{rel}^{exp}/u_c^{pred} > 1$ for all but a few bouncing collisions. Therefore, Eq. (6) and the parameters in Table 1 could be used to predict the critical velocity in the coalescence kernel function of Lehr et al. [24] for the simulation of gas–liquid contactors operating with the liquids considered in this work.

Since Eq. (6) is able to represent the experimental data, we shall now utilise it to further illustrate the effect of electrolytes on the critical velocity. For each operating temperature, a comparison is drawn in Fig. 9 between the u_c values predicted with Eq. (6) for water and the two NaCl solutions, based on the parameters listed in Table 1. In order to enable a direct comparison between individual graphs, the same scale was adopted for all plots presented in Fig. 9. In perfect agreement with the coalescence hindrance effect of electrolytes, regardless of the equivalent bubble diameter, the critical velocity for bubble coalescence decreases as the NaCl concentration increases. It is interesting to observe, in particular, that the absolute drop in u_c does not depend on d_e, and hence the electrolyte addition actually leads to a translation of the curve related to water towards lower values. Whatever the mechanism for coalescence hindrance may be, the reduction in the critical velocity demonstrates that the presence of electrolytes requires a longer interacting time between approaching bubbles for coalescence to take place, which could be a result of an increase in the time for draining the liquid film between the bubbles.

Upon comparing Fig. 9a–d, one notices that the extent of the electrolyte effect for a given concentration seems to decrease as the operating temperature is raised, since the individual curves become progressively closer to each other. Consequently, it can be concluded that the presence of electrolytes and the liquid temperature have opposite effects on bubble coalescence. In particular, focusing on the region of constant critical velocity, it is clear that, for a given liquid phase, the u_c value grows with the liquid temperature, which is a further evidence of the enhancement of bubble coalescence with increasing temperature recently reported by Ribeiro and Mewes [22]. Any suitable mechanism to describe the effect of electrolytes on bubble coalescence should be consistent with all these experimental behaviours. Deschenes et al. [13] have stated that none of the available mechanisms [5,9–12,44] could account for their experimental observations and proposed a new approach to explain the effect of electrolytes in terms of their influence on the free energy of the bulk liquid in the film or on that of the vapour–liquid interface. The coalescence hindrance would be a result of the increase in the vaporisation energy of the film due to the presence of the

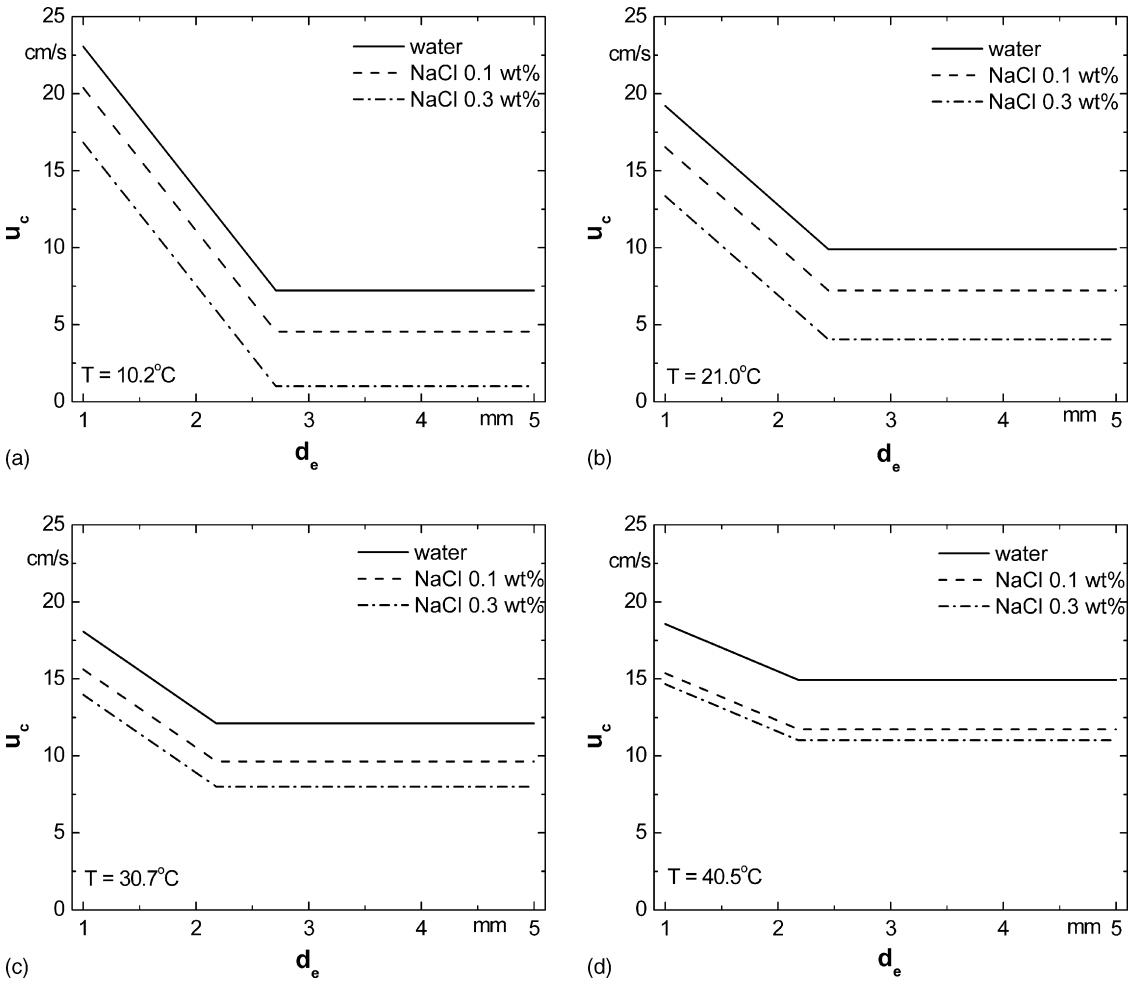

Fig. 9. Critical velocities as a function of the equivalent diameter of the colliding bubbles predicted with Eq. (6) for water and NaCl solutions at different operating temperatures: (a) 10.2 °C; (b) 21.0 °C; (c) 30.7 °C; (d) 40.5 °C.

electrolyte, assuming that the vaporisation would be related to the film rupture. Considering that the enthalpy of vaporisation decreases with temperature, this reasoning does also agree with the augmentation of bubble coalescence with the liquid temperature experimentally observed in this work.

4. Conclusions

Bubbles collisions in water and NaCl solutions at four different temperatures were recorded with the aid of a high-speed video camera in order to investigate the effect of dissolved electrolytes upon the critical velocity for bubble coalescence.

Previous authors' conclusion of a critical velocity independent of the equivalent diameter of the colliding bubbles was shown to be only partially valid. As the bubble diameter becomes smaller, a point is reached at which the critical velocity starts to increase linearly with decreasing equivalent diameter. This behaviour seems to be related to the importance of bubble deformation in the film-drainage process and the distinction between the two different regions was associated with the minimum bubble diameter required for the formation of the characteristic liquid film shape known as the dimple. Regardless of the liquid composition, in the region of variable critical velocity, the effect of the equivalent diameter decreased as the liquid temperature was raised.

In agreement with the coalescence hindrance effect reported in the literature for most electrolytes, regardless of the liquid temperature, the critical velocity decreased with the addition of NaCl into water. Moreover, the absolute decrease was independent of the equivalent diameter, so that the curve for water was actually translated towards lower values as the concentration of NaCl increased, an effect whose extent for a given concentration decreased with the liquid temperature. For both water and the NaCl solutions, bubble coalescence was enhanced with increasing liquid temperature and the critical velocity values grew accordingly.

An empirical equation including three parameters was proposed to describe the experimentally observed trends. The first parameter can be interpreted as the minimum bubble diameter required for bubble deformation to play an important role in the film thinning process, whereas the second one is a lumped parameter to account for all processes which lead to the influence of the equivalent diameter on the critical velocity. Both parameters were only temperature-dependent within the NaCl

concentrations adopted. The third and last parameter accounts for the electrolyte effect and varied with both the liquid temperature and the concentration of electrolytes.

It should be emphasised that there are, however, electrolytes which do not seem to influence bubble coalescence. The facts observed with NaCl in this study may only be extrapolated to other electrolytes that are known to inhibit bubble coalescence.

Acknowledgement

Dr. C.P. Ribeiro Jr. would like to thank the Alexander von Humboldt Foundation for the research fellowship (IV-BRA/1118568).

References

[1] R.V. Chaudhari, H. Hofmann, Coalescence of gas bubbles in liquids, Rev. Chem. Eng. 10 (1994) 131–190.
[2] V.S.J. Craig, Bubble coalescence and specific-ion effects, Curr. Opin. Colloid Interface Sci. 9 (2004) 178–184.
[3] J. Zahradnik, M. Fialova, M. Ruzicka, J. Drahos, F. Kastanek, N.H. Thomas, Duality of the gas–liquid flow regimes in bubble column reactors, Chem. Eng. Sci. 52 (1997) 3811–3826.
[4] C.P. Ribeiro Jr., P.L.C. Lage, Gas–liquid direct-contact evaporation: a review, Chem. Eng. Technol. 28 (2005) 1081–1107.
[5] G. Marrucci, A theory of coalescence, Chem. Eng. Sci. 24 (1969) 975–985.
[6] P.-S. Hahn, J.-D. Chen, J.C. Slattery, Effects of London-van der Waals forces on the thinning and rupture of a dimpled liquid film as a small drop or bubble approaches a fluid–fluid interface, AIChE J. 31 (1985) 2026–2038.
[7] T.O. Oolman, H.W. Blanch, Bubble coalescence in stagnant liquids, Chem. Eng. Commun. 43 (1986) 237–261.
[8] D. Li, S. Liu, Coalescence between small bubbles or drops in pure liquids, Langmuir 12 (1996) 5216–5220.
[9] R.R. Lessard, S.A. Zieminski, Bubble coalescence and gas transfer in aqueous electrolytic solutions, Ind. Eng. Chem. Fundam. 10 (1971) 260–269.
[10] V.S.J. Craig, B.W. Ninham, R.M. Pashley, The effect of electrolytes on bubble coalescence in water, J. Phys. Chem. 97 (1993) 10192–10197.
[11] P.K. Weissenborn, R.J. Pugh, Surface tension and bubble coalescence phenomena of aqueous solutions of electrolytes, Langmuir 11 (1995) 1422–1426.
[12] S.J. Miklavcic, Deformation of fluid interfaces under double-layer forces stabilizes bubble dispersions, Phys. Rev. E 54 (1996) 6551–6556.
[13] L.A. Deschenes, J. Barrett, L.J. Muller, J.T. Fourkas, U. Mohanty, Inhibition of bubble coalescence in aqueous solutions. I. Electrolytes, J. Phys. Chem. B 102 (1998) 5115–5119.
[14] R.S. Allan, G.E. Charles, S.G. Mason, The approach of gas bubbles to a gas–liquid interface, J. Colloid Sci. 16 (1961) 150–165.
[15] F.W. Cain, J.C. Lee, A technique for studying the drainage and rupture of unstable liquid films formed between two captive bubbles: measurements on KCl solutions, J. Colloid Interface Sci. 106 (1985) 70–85.
[16] L. Doubliez, The drainage and rupture of a non-foaming liquid film formed upon bubble impact with a free surface, Int. J. Multiphase Flow 17 (1991) 783–803.
[17] K. Ueyama, M. Saeki, M. Matsukata, Development of system for measuring bubble coalescence time by using a laser, J. Chem. Eng. Jpn. 26 (1993) 308–314.
[18] R.D. Kirkpatrick, M.J. Lockett, The influence of approach velocity on bubble coalescence, Chem. Eng. Sci. 29 (1974) 2363–2373.
[19] A.K. Chesters, G. Hofman, Bubble coalescence in pure liquids, Appl. Scient. Res. 38 (1982) 353–361.
[20] P.C. Duineveld, Bouncing and coalescence of bubble pairs rising at high Reynolds number in pure water or aqueous surfactant solutions, Appl. Scient. Res. 58 (1998) 409–419.
[21] T. Sanada, M. Watanabe, T. Fukano, Effects of viscosity on coalescence of a bubble upon impact with a free surface, Chem. Eng. Sci. 60 (2005) 5372–5384.
[22] C.P. Ribeiro Jr., D. Mewes, On the effect of liquid temperature upon bubble coalescence, Chem. Eng. Sci. 61 (2006) 5704–5716.
[23] D. Wiemann, Numerical Calculation of Flow and Concentration Fields in Two- and Three-phase Bubble Columns, PhD Thesis. University of Hannover, Germany, 2005, 118p. (in German).
[24] F. Lehr, M. Milies, D. Mewes, Bubble-size distributions and flow fields in bubble columns, AIChE J. 48 (2002) 2426–2443.
[25] M.J. Prince, H.W. Blanch, Bubble coalescence and break-up in air-sparged bubble columns, AIChE J. 36 (1990) 1485–1499.
[26] D. Colella, D. Vinci, R. Bagatin, M. Masin, E.A. Bakr, A study on coalescence and breakage mechanisms in three different bubble columns, Chem. Eng. Sci. 54 (1999) 4767–4777.
[27] K. Shimizu, S. Takada, K. Minekawa, Y. Kawase, Phenomenological model for bubble column reactors: prediction of gas hold-ups and volumetric mass transfer coefficients, Chem. Eng. J. 78 (2000) 21–28.
[28] C.P. Ribeiro Jr., P.L.C. Lage, Population balance modelling of bubble size distributions in a direct-contact evaporator using a sparger model, Chem. Eng. Sci. 59 (2004) 2363–5377.
[29] G. Marrucci, L. Nicodemo, Coalescence of gas bubbles in aqueous solutions of inorganic electrolytes, Chem. Eng. Sci. 22 (1967) 1257–1265.
[30] G. Keitel, U. Onken, Inhibition of bubble coalescence by solutes in air/water dispersions, Chem. Eng. Sci. 37 (1982) 1635–1638.
[31] J.W. Kim, J.H. Chang, W.K. Lee, Inhibition of bubble coalescence by electrolytes, Korean J. Chem. Eng. 7 (1990) 100–108.
[32] M. Millies, D. Mewes, Interfacial area in bubble flow. 3. Coalescence inhibition, Chem. Ing. Technol. 68 (1996) 927–933 (in German).
[33] J. Zahradnik, M. Fialova, V. Linek, The effect of surface-active additives on bubble coalescence in aqueous media, Chem. Eng. Sci. 54 (1999) 4757–4766.
[34] W.S. Rasband, ImageJ US, National Institutes of Health, Bethesda, Maryland, USA, 1997, http://rsb.info.nih.gov/ij/.
[35] G. Drogaris, P. Weiland, Studies of coalescence of bubble pairs, Chem. Eng. Commun. 23 (1983) 11–26.
[36] T.D. Hodgson, J.C. Lee, The effect of surfactants on the coalescence of a drop at an interface, J. Colloid Interface Sci. 30 (1969) 94–108.
[37] G. Drogaris, P. Weiland, Coalescence behaviour of gas bubbles in aqueous solutions of *n*-alcohols and fatty acids, Chem. Eng. Sci. 38 (1983) 1501–1506.
[38] J.B.W. Kok, Dynamics of a pair of gas bubbles moving through liquid. II. Experiment, Eur. J. Mech. B 4 (1993) 541–560.
[39] R. Clift, J.R. Grace, M.E. Weber, Bubbles, Drops and Particles, Academic Press, New York, 1978, p. 172.
[40] Y.H. Tsang, Y.-H. Koh, D.L. Koch, Bubble-size dependence of the critical electrolyte concentration for inhibition of coalescence, J. Colloid Interface Sci. 275 (2004) 290–297.
[41] G.E. Charles, S.G. Mason, The coalescence of liquid drops with flat liquid–liquid interfaces, J. Colloid Sci. 15 (1960) 236–267.
[42] A. Smolianski, H. Haario, P. Luukka, Vortex shedding behind a rising bubble and two-bubble coalescence: a numerical approach, Appl. Math. Modell. 29 (2005) 615–632.
[43] P.K. Weissenborn, R.J. Pugh, Surface tension of aqueous solutions of electrolytes: relationship with ion hydration, oxygen solubility and bubble coalescence, J. Colloid Interface Sci. 184 (1996) 550–563.
[44] H.K. Christenson, V.V. Yaminsky, Solute effects on bubble coalescence, J. Phys. Chem. 99 (1995) 10420.